

Gamma Ray Bursts as cosmological tools

G. Ghirlanda*, G. Ghisellini*, L. Nava* and C. Firmani^{*,†}

^{*}*Osservatorio Astronomico di Brera, Via E. Bianchi 46 I-23807 Merate*

[†]*Instituto de Astronomia U.N.A.M., A.P. 70-264, 04510, Mexico, D.F., Mexico*

Abstract. The use of Gamma Ray Bursts as “standard candles” has been made possible by the recent discovery of a very tight correlation between their rest frame intrinsic properties. This correlation relates the GRB prompt emission peak spectral energy E_{peak} to the energy E_{γ} corrected for the collimation angle θ_{jet} of these sources. The possibility to use GRBs to constrain the cosmological parameters and to study the nature of Dark Energy are very promising.

Keywords: gamma-ray sources; gamma-ray bursts; Observational cosmology

PACS: 98.70.Rz,98.80.Es

INTRODUCTION

The extremely large luminosity of Gamma Ray Bursts (GRBs) makes them detectable, in principle, out to very large redshifts $z < 20$ (e.g. [1]). The present redshift distribution for ~ 60 GRBs, which extends out to $z = 6.29$ for GRB 050904 ([2]) would make GRBs exquisite potential tools for observational cosmology. They can have a profound impact on: (i) the study the epoch of re-ionization; (ii) the characterization of the properties of the cosmic intervening medium; (iii) the study of the cosmic star formation history back to unprecedented epochs; (iv) the description of the geometry of the Universe and (v) the investigation of the nature of Dark Energy (DE).

However, the last two points require a class of “standard candles” whose spread in the Hubble diagram is comparable (and even smaller) than the precision on the measure of their luminosity distance. At first glance GRBs are everything but standard candles: their intrinsic isotropic emitted energies span more than 4 orders of magnitudes, and even the collimation corrected energy span about two orders of magnitudes. This has prevented, until recently, their application as cosmological tools ([4]; [5]; [6])

However, the discovery of a very tight (so called “Ghirlanda”) correlation, with a scatter less than 0.1 dex, between the rest frame spectral peak energy E_{peak} and the collimation corrected energy E_{γ} ([7]) allowed a very accurate measurement of the true GRB energetics and made them usable as “standard candles” to constrain the cosmological parameters $\Omega_M, \Omega_{\Lambda}$ and to study the DE equation of state ([8, 9]).

There are some issues to be discussed about the use of the Ghirlanda correlation for cosmology and the existence of the $E_{\text{peak}}-E_{\gamma,\text{iso}}$ correlation (so called “Amati” ref [3]).

The cosmological use of the $E_{\text{peak}}-E_{\gamma}$ correlation suffers from the so called “circularity” problem ([7], see also [10]) due to the fact that the correlation is not calibrated with (for instance) low redshift GRBs and, therefore, its slope and normalization are cosmology dependent. The latter problem could be solved with either a number of low redshift

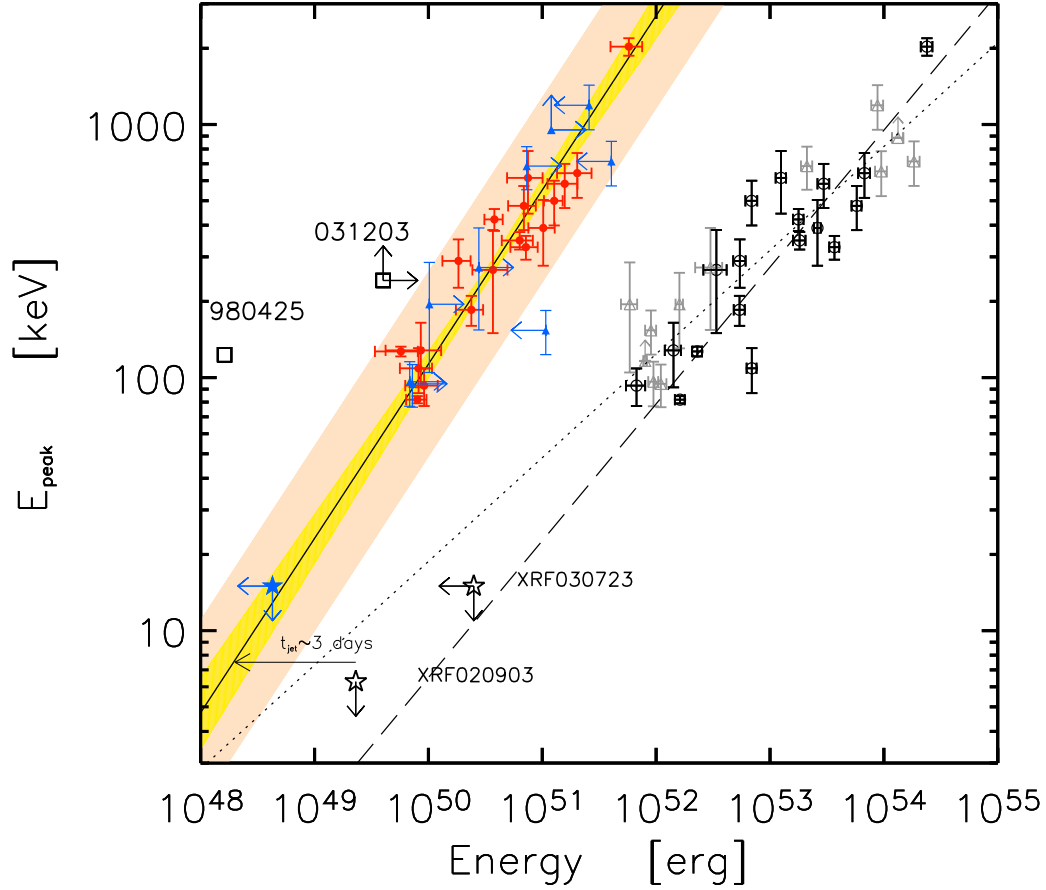


FIGURE 1. Rest frame peak energy E_{peak} versus isotropic (open symbols) and collimation corrected (filled symbols) energy. The black open circles are the 18 GRBs ([19]) with measured z , E_{peak} and t_{jet} for which the collimation corrected energy could be computed (red filled circles). Upper/lower limits on either one of the variables are shown by the blue filled triangles. The best fit powerlaw to the red filled circles (Eq. 1) is represented by the solid (blue) line and its uncertainty by the thin yellow shaded region. The large (light orange) shaded region represents the 3σ gaussian scatter of the data points around the correlation. Also shown is the Amati correlation obtained by fitting the open black data points and the open grey triangles (which are not upper/lower limits) either accounting for the errors on both the coordinates (long dashed line - slope = 0.54 and $\chi_r^2 = 8.4$ for 26 dof) and by a linear regression (dotted line - slope = 0.4). Note the two XRF (030723 and 020903) and the two GRBs 980425/SN1998bw and 031203/SN2003lw which are outliers with respect to both the Ghirlanda and the Amati correlations.

GRBs or through a convincing theoretical interpretation (see [11, 12], [13] and [14]) for possible interpretations) fixing at least its slope. In the meanwhile different approaches have been adopted ([8, 9]) to circumvent this problem.

The Amati correlation was derived with a very limited sample of GRBs (originally only 9 [3], then 24 [7]) and it is possible that it is affected by some selection effect connected to the need to have a measured spectroscopic redshift (which may select the

brightest bursts). While these possible selection effects are still a matter of debate, this correlation (as well as the Ghirlanda one) appears to be satisfied by the (few) newly discovered HETE-II and Swift GRBs. Furthermore, more sophisticated statistical tests, based on the large BATSE sample of GRBs ([15, 16] and [17, 18]), have been performed.

THE $E_{\text{PEAK}} - E_{\gamma}$ CORRELATION IN LONG GRB

The $E_{\gamma} - E_{\text{peak}}$ correlation is found with all the GRBs with (i) a secure (spectroscopic) redshift measurement, (ii) well known prompt emission spectral properties and (iii) a measured jet break time (from the afterglow light curve). The latter, in fact, allows to derive, within the standard GRB scenario, the burst opening angle θ_{jet} and to compute the collimation corrected energy $E_{\gamma} = E_{\text{iso}}(1 - \cos \theta)$.

Since the publication of the initial sample of 15 GRBs [7] there have been 3 new GRBs with all the three input parameters measured. Furthermore, some spectral data have been slightly revised for the old GRBs. Then the sample now contains 18 GRBs (updated to August 2005) with measured z , E_{peak} and t_{jet} . This sample is presented and discussed in details in [19]. In the uniform jet model with a uniform density circumburst medium, the updated Ghirlanda correlation becomes:

$$\left(\frac{E'_{\text{p}}}{100 \text{keV}} \right) = (2.79 \pm 0.15) \left(\frac{E_{\gamma}}{2.72 \times 10^{50} \text{erg}} \right)^{0.69 \pm 0.04} \quad (1)$$

with a reduced $\chi^2_{\text{r}} = 1.4$ (16 dof). This correlation and the data points (solid line and red-filled circles, respectively) are shown in Fig. 1 together with the updated Amati correlation (long dashed line). The data points (red filled circles) have a gaussian scatter with $\sigma = 0.1$ (the 3σ scatter is represented by the light shaded region in Fig. 1) around the correlation represented by Eq. 1. Both the scatter and the slope of this updated Ghirlanda correlation are consistent with what found with the sample of 15 bursts of [7].

With this updated Ghirlanda correlation (Eq. 1) we fitted the cosmological parameters $\Omega_M, \Omega_{\Lambda}$ and w_0, w_a with the bayesian method proposed in [9] and found results fully consistent with those presented in [9].

THE JET OPENING ANGLE DISTRIBUTION OF GRBS

The Ghirlanda correlation is derived by correcting the isotropic equivalent energies $E_{\gamma, \text{iso}}$ for the collimation angle θ_{jet} . In [7] (see also [17]) it was demonstrated that the scatter of the Amati correlation can be interpreted as due entirely to the different jet opening angles (see also Fig. 1 of [9]). Still, it has been argued ([15, 16]) that the Amati correlation might be only a selection effect because inconsistent with the largest population of GRBs detected by BATSE. We performed ([17] see also [18]) a different test by checking if a large sample of GRBs with a pseudo-redshift estimate could indicate the existence of a relation in the $E_{\text{peak}} - E_{\gamma, \text{iso}}$ plane.

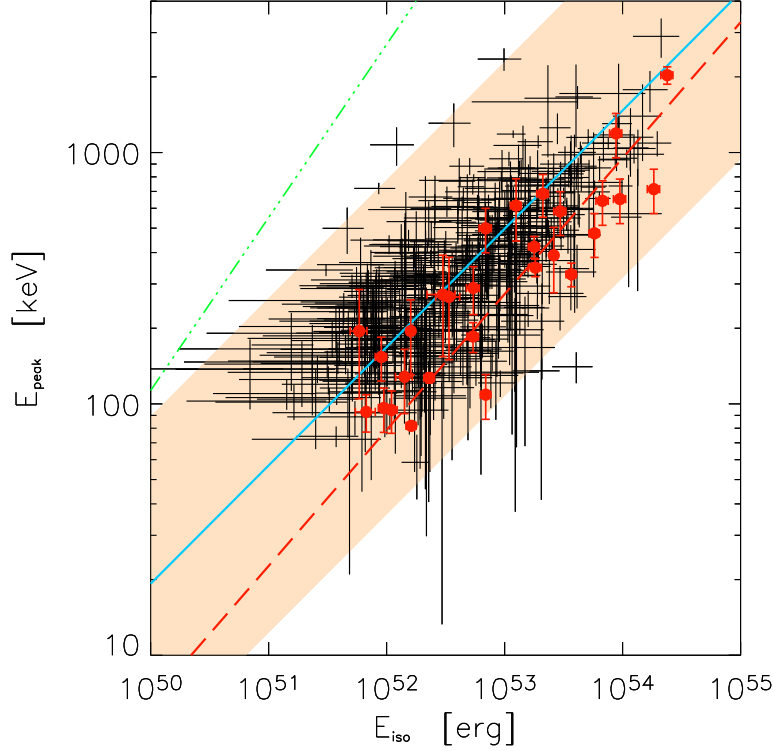


FIGURE 2. Rest frame peak energy E_{peak} versus isotropic equivalent energy $E_{\gamma,\text{iso}}$. Red filled circles are the 28 GRBs with spectroscopically measured redshifts and published spectral properties. The long-dashed line is their best fit (weighting for the errors on both variables) which is $E_{\text{peak}} \propto E_{\gamma,\text{iso}}^{0.54}$ with a reduced $\chi_r^2 = 8.4$ (26 dof). The black crosses are the 442 GRBs with pseudo redshifts derived from the lag–luminosity relation. The solid line is the best fit to these data points which gives $E_{\text{peak}} \propto E_{\gamma,\text{iso}}^{0.47}$ with a reduced $\chi_r^2 = 4.0$ (440 dof). The shaded area represents the 3σ scatter region of the black points around their best fit line (solid line). The triple-dot-dashed line is the Ghirlanda correlation (Eq. 1).

With a sample of 442 long duration GRBs whose spectral properties has been studied ([20]) and whose redshifts has been derived from the lag–luminosity relation ([21]), we populated the $E_{\text{peak}} - E_{\gamma,\text{iso}}$ plane (black crosses in Fig. 2). We found that this large sample of bursts produces an Amati correlation (solid line in Fig. 2) whose slope (normalization) is slightly flatter (larger) than that found with the sample of 28 GRBs (red filled circles in Fig. 2). The gaussian scatter of the 442 bursts around their correlation has a standard deviation $\sigma = 0.22$, i.e. fully consistent with that of the 28 GRBs around their best fit correlation (long-dashed red line in Fig. 2). This suggests that a relation between E_{peak} and $E_{\gamma,\text{iso}}$ does exist.

However, it might still be argued that the correlation found with the 28 and with the 442 GRBs have different normalizations, although similar scatter and slopes. This is evident from the relative position of the 28 GRBs (red filled circles in Fig. 2): they

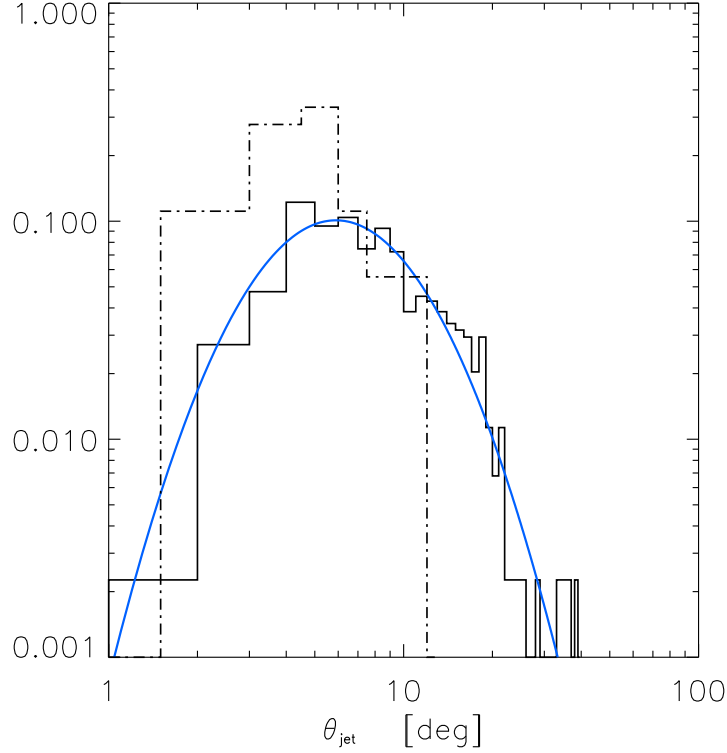


FIGURE 3. Jet opening angle distributions. The solid line histogram represents the θ_{jet} derived from the large sample of 442 GRBs with pseudo redshifts requiring that they satisfy the Ghirlanda relation as represented by Eq. 1. The solid line is the best fit log-normal distribution. The dot-dashed histogram represents the angle distribution of the 18 GRBs with spectroscopic redshifts and well constrained t_{jet} .

lie on the right tail of the scatter distribution of the 442 GRBs (black crosses) in the $E_{\text{peak}} - E_{\gamma,\text{iso}}$ plane. This can be easily interpreted as due to a selection effect. In fact, we can derive the jet opening angle of the 442 GRBs by assuming that the Ghirlanda correlation exists and that its scatter is (as shown in [7, 9]) much smaller than that of the Amati correlation. The angle distribution is shown in Fig. 3 (solid histogram) and it is well represented by a log-normal distribution (solid line) with a typical $\theta_{\text{jet}} \sim 6^\circ$. The angle distribution of the 28 GRBs with measured t_{jet} is also shown (dot-dashed histogram in Fig. 3) and it is shifted to the small-angle tail of the θ_{jet} distribution of the other 442 bursts. This suggests that the 28 GRBs which are used to define the Amati correlation have jet opening angles which are systematically smaller than average. This makes them more luminous and brighter. In turn, this makes them better candidates to have an optical follow up and to have their redshift measured.

We conclude that the origin of the Amati correlation is connected to: i) the existence of the Ghirlanda correlation and ii) the existence of a *peaked* jet opening angle distribution. Were it flat, then the $E_{\gamma,\text{iso}} - E_{\text{peak}}$ correlation would not exist.

ACKNOWLEDGMENTS

We thank the LOC and SOC for this stimulating conference. We thank A. Celotti, F. Tavecchio, D. Lazzati and D. Lamb for useful discussions.

REFERENCES

1. D. Lamb & D. Reichart, *The Astrophysical Journal*, **536**, 1 (2000)
2. A. Antonelli, et al., *GCN*, 3924 (2005)
3. L. Amati, et al. *The Astrophysical Journal*, **390**, 81 (2002)
4. J. S. Bloom, D. A. Frail & R. Sari, *Astrophysical Journal*, **121**, 2879 (2001)
5. D. A. Frail et al., *The Astrophysical Journal Letters*, **526**, L55 (2001)
6. B. E. Schaefer, *The Astrophysical Journal Letters*, **583**, L67 (2003)
7. G. Ghirlanda, G. Ghisellini & D. Lazzati, *The Astrophysical Journal*, **616**, 331 (2004)
8. G. Ghirlanda, G. Ghisellini, D. Lazzati & C. Firmani *The Astrophysical Journal Letters*, **613**, L13 (2004)
9. C. Firmani, G. Ghisellini, G. Ghirlanda & V. Avila-Reese, *Montly Notices of The Royal Astronomical Society*, **360**, L1 (2005)
10. G. Ghisellini et al., *Il Nuovo Cimento* in press, astro-ph/0504306 (2005)
11. D. Eichler & A. Levison, *The Astrophysical Journal*, **614**, L13 (2004)
12. A. Levinson & D. Eichler, *The Astrophysical Journal*, **629**, L13 (2005)
13. R. Yamazaki, K. Ioka, T. Nakamura, *The Astrophysical Journal*, **606**, L33 (2004)
14. M.J. Rees & P. Meszaros, *The Astrophysical Journal*, **628**, 847 (2005)
15. E. Nakar & T. Piran, *Montly Notices of The Royal Astronomical Society*, **360**, L73 (2005)
16. D. L. Band & R. D. Preece, *The Astrophysical Journal*, **627**, 319 (2005)
17. G. Ghirlanda, G. Ghisellini & C. Firmani *Montly Notices of The Royal Astronomical Society*, **361**, L10 (2005)
18. Z. Bosnjak et al., *Montly Notices of The Royal Astronomical Society*, in press, astro-ph/0502185 (2005)
19. L. Nava et al., *Montly Notices of The Royal Astronomical Society*, submitted, (2005)
20. D. Yonetoku et al., *The Astrophysical Journal*, **609**, 935 (2004)
21. D. L. Band, J. P. Norris, J. T. Bonnel, *The Astrophysical Journal*, **613**, 848 (2004)